

# Spiral-type terahertz antennas and the manifestation of the Mushiake principle

Ranjan Singh<sup>1</sup>, Carsten Rockstuhl<sup>2</sup>, Christoph Menzel<sup>2</sup>, Todd P. Meyrath<sup>3</sup>, Mingxia He<sup>1,4</sup>, Harald Giessen<sup>3</sup>, Falk Lederer<sup>2</sup>, and Weili Zhang<sup>1</sup>

<sup>1</sup>School of Electrical and Computer Engineering, Oklahoma State University, Stillwater, Oklahoma 74078, USA

<sup>2</sup>Institut für Festkörpertheorie und -optik, Friedrich-Schiller-Universität Jena, D-07743, Jena, Germany

<sup>3</sup>Physikalisches Institut, Universität Stuttgart, D-70550 Stuttgart, Germany

<sup>4</sup>Center for Terahertz waves and College of Precision Instrument and Optoelectronics Engineering, Tianjin University, and the key Laboratory of Optoelectronics Information and Technical Science (Ministry of Education), Tianjin 300072, Peoples Republic of China

[weili.zhang@okstate.edu](mailto:weili.zhang@okstate.edu)

**Abstract:** We report on the experimental and theoretical study of the resonant eigenmodes of spiral-type terahertz antennas. The analysis is carried out for a varying number of spiral windings. For larger numbers the structure possesses a self-complementary property which allows the application of the Mushiake principle predicting that the impedance of such structures is half the impedance of free space. This permits to observe an equal and frequency independent reflection and transmission coefficient. This property makes the spiral-type terahertz antenna not only a fascinating example of a medium supporting strong resonances in the long wavelength limit but also a medium which can be easily and reasonably homogenized at higher frequencies. This is in stark contrast to most of the existing metamaterials.

© 2009 Optical Society of America

**OCIS codes:** (160.4670) Optical materials; (240.6680) Surface plasmons; (260.3910) Metal optics; (260.5740) Resonance

---

## References and links

1. P. Mühllegel, H.-J. Eisler, O. J. F. Martin, B. Hecht, and D. W. Pohl, "Resonant Optical Antennas," *Science* **308** 1607–1609 (2005).
2. R. D. Grober, R. J. Schoelkopf, and D. E. Prober, "Optical antenna: Towards a unity efficiency near-field optical probe," *Appl. Phys. Lett.* **70** 1354–1356 (1997).
3. L. Novotny, B. Hecht, *Principles of Nano-Optics*, 1st edn. (Cambridge University Press, 2006).
4. R. Singh, E. Smirnova, A. J. Taylor, J. F. OHara, and W. Zhang, "Optically thin terahertz metamaterials," *Opt. Express* **16** 65376543 (2008).
5. T. H. Taminiua, F. D. Stefani, F. B. Segerink, and N. F. van Hulst, "Optical antennas direct single-molecule emission," *Nature Photonics* **2** 234–237 (2008).
6. K. B. Crozier, A. Sundaramurthy, G. S. Kino, and C. F. Quate, "Optical antennas: Resonators for local field enhancement," *J. Appl. Phys.* **94** 4632–4642 (2003).
7. P. Bharadwaj and L. Novotny, "Spectral dependence of single molecule fluorescence enhancement," *Opt. Express* **15** 14266–14274 (2007).
8. N. Engheta, R. W. Ziolkowski, *Electromagnetic Metamaterials: Physics and Engineering Aspects*, 1st edn. (Wiley & Sons, 2006).
9. T. Zentgraf, J. Dorfmüller, C. Rockstuhl, C. Etrich, R. Vogelgesang, K. Kern, T. Pertsch, F. Lederer, and H. Giessen, "Amplitude- and phase-resolved optical near fields of split-ring resonator based metamaterials," *Opt. Lett.* **33** 848–850 (2008).

10. D. J. Cho, F. Wang, X. Zhang, and Y. Ron Shen, "Contribution of the electric quadrupole resonance in optical metamaterials," *Phys. Rev. B* **78** 121101(R) (2008).
11. D. Seetharamdoo, R. Sauleau, K. Mahdjoubi, and A.-C. Tarot, "Effective parameters of resonant negative refractive index metamaterials: Interpretation and validity," *J. Appl. Phys.* **98** 063505 (2005).
12. C. Rockstuhl, C. Menzel, T. Paul, T. Pertsch, and F. Lederer, "Light propagation in a fishnet metamaterial," *Phys. Rev. B* **78** 155102 (2008).
13. E. Prodan and P. Nordlander, "Plasmon hybridization in spherical nanoparticles," *J. Chem. Phys.* **120** 5444–5454 (2007).
14. N. Liu, S. Kaiser, and H. Giessen, "Magnetoinductive and Electroinductive Coupling in Plasmonic Metamaterial Molecules," *Adv. Matter.* **20** 4521–4525 (2008).
15. M. I. Stockman, S. V. Faleev, and D. J. Bergman, "Coherent Control of Femtosecond Energy Localization in Nanosystems," *Phys. Rev. Lett.* **88** 067402 (2002).
16. T. Brixner, F. J. García de Abajo, J. Schneider, C. Spindler, and W. Pfeiffer, "Ultrafast adaptive optical near-field control," *Phys. Rev. B* **73** 125437 (2006).
17. Y. Mushikake, *Self-Complementary Antennas. Principle of Self-Complementarity for Constant Impedance*, 1st edn. (Springer, 1996)
18. Y. Mushikake, "Self-complementary antennas," *IEEE Antennas and Propagation Magazine*, **34** 23–29 (1992).
19. K. A. McIntosh, E. R. Brown, K. B. Nichols, O. B. McMahon, W. F. DiNatale, and T. M. Lyszczarz, "Terahertz photomixing with diode lasers in low-temperature-grown GaAs," *Appl. Phys. Lett.* **67** 3844–3846 (1995).
20. J. F. OHara, R. Singh, I. Brener, E. Smirnova, J. Han, A. J. Taylor, and W. Zhang, "Thin film sensing with planar terahertz metamaterials:sensitivity and limitations," *Opt. Express* **16** 1786-1795 (2008).
21. D. Grischkowsky, S. Keiding, M. van Exter, and Ch. Fattinger, "Far-infrared time-domain spectroscopy with terahertz beams of dielectrics and semiconductors," *J. Opt. Soc. Am. B* **7** 2006–2015 (1990).
22. R. Singh, C. Rockstuhl, F. Lederer, and W. Zhang, "Coupling between a dark and a bright eigenmode in a terahertz metamaterial," *Phys. Rev. B* **79** 085111 (2009).
23. Abul K. Azad, J. Dai, and W. Zhang, "Transmission properties of terahertz pulses through subwavelength double split ring resonators," *Opt. Lett.* **31** 634636 (2006).
24. L. Li, "New formulation of the Fourier modal method for crossed surface-relief gratings," *J. Opt. Soc. Am. A* **14**, 2758-2767 (1997).
25. M. A. Ordal, L. L. Long, R. J. Bell, S. E. Bell, R. R. Bell, R. W. Alexander, Jr., and C. A. Ward, "Optical properties of the metals Al, Co, Cu, Au, Fe, Pb, Ni, Pd, Pt, Ag, Ti, and W in the infrared and far infrared," *Appl. Opt.* **22**, 1099-1119 (1983).
26. A. Papakostas, A. Potts, D. M. Bagnall, S. L. Prosvirnin, H. J. Coles, and N. I. Zheludev, "Optical Manifestations of Planar Chirality," *Phys. Rev. Lett.* **90** 107404 (2003).
27. T. Vallius, K. Jefimovs, J. Turunen, P. Vahimaa, and Y. Svirko, "Optical activity in subwavelength-period arrays of chiral metallic particles," *Appl. Phys. Lett.* **83** 234 (2003).
28. C. Menzel, C. Rockstuhl, T. Paul, and F. Lederer, "Retrieving effective parameters for quasiplanar chiral metamaterials," *Appl. Phys. Lett.* **93**, 233106 (2008).
29. R. Esteban, R. Vogelgesang, J. Dorfmüller, A. Dmitriev, C. Rockstuhl, C. Etrich, and K. Kern, "Direct near-field optical observation of higher order plasmonic resonances," *Nano Letters* **8**, 3155–3159 (2008).

## 1. Introduction

Metallic optical antennas either permit the localization of light from an external source within tiny volumes or facilitate the radiation of a localized light source into the far-field [1]. Such radiation tends to be significantly enhanced and/or strongly directed [2]. This property renders them suitable as building blocks for a large variety of applications in the field of nanoplasmonics [3]. The peculiarities of optical antennas predominantly arise from the excitation of plasmonic eigenmodes in these structures [4], which dominate the scattering properties of the optical system at resonance [5]. In most cases, a sufficient size for the metallic antennas is required to ensure an appropriate scattering strength and/or to sustain the eigenmodes with a desired field distribution [6]. If the optical antenna dimensions are small when compared to the relevant wavelength, its scattering properties may be described in the electrostatic limit [7] where only electric dipole resonances may be excited.

By contrast, metallic optical antennas can also be understood as being the prototypical building blocks for metamaterials [8]. Likewise, by exploiting the excitation of resonant eigenmodes in an appropriately shaped metallic antenna, a peculiar scattering response is achieved [9]. The periodic arrangement of such optical antennas mimics naturally available materials. The natu-

ral material as well as the metamaterial can conceptually be understood as being composed of polarizable entities. By varying the geometry of the optical antenna, the scattered field of the eigenmodes can be controlled. In the past geometries were put forward, which exhibited scattering responses dominated either by an electric dipole, a magnetic dipole or even higher order multipole moments [10]. As a rule of thumb, one is inclined to believe that for sufficiently small unit cells, light will not resolve the spatial details of the structure but merely experience an effective medium [11]. More rigorously, the homogenization requires the dominance of the fundamental Bloch mode which essentially resembles a plane wave in a homogeneous medium[12].

Although one aims at different applications of nanoplasmonics the primary aim is usually to control the plasmonic eigenmodes of metallic antennas. This goal led to the implementation of various approaches to extend the choice of structures at hand. One example might be the rational approach of plasmon hybridization [13], where a number of single plasmonic antennas is strongly coupled. The resulting scattering properties of the complex system may be explained by the appearance of bonding and anti-bonding states [14]. Another example might be a rather heuristic approach of coherent control [15] where complex optical antennas are used to sustain unspecified plasmonic eigenmodes. Controlling their excitation with shape optimized pulses using e.g. genetic algorithms, led to a desired field distribution due to a coherent superposition of the excited eigenmodes [16].

Along these lines of research here we aim at systematically revealing the optical properties of metallic antennas with an increasing degree of complexity. The geometry of the optical antennas under consideration is that of a spiral. The optical properties are analyzed for antennas with an increasing number of windings. First, we are concerned with an analysis of the respective plasmonic eigenmodes where we reveal a peculiarity compared to the properties of most contemporary antennas which are used as building blocks for metamaterials. We show that the spiral-type antenna sustains strong resonances in the long wavelength limit. Moreover, an ensemble of such antennas can be fairly trivially homogenized for shorter wavelengths being a direct consequence of the Mushiake principle, originally introduced for antennas operating at radio frequencies [17]. It states that the impedance of a self-complementary antenna amounts to half of the free space impedance. This unique property leads to identical reflection and transmission coefficients over a large spectral domain, a property which has enabled numerous applications at radio frequencies [18]. Besides characterizing the resonance properties of such spiral type antennas, it is therefore the aim of this contribution to reveal the implication of the Mushiake principle for optical antennas and to discuss its potential applications. We note that similar spiral antennas were already implemented at terahertz (THz) frequencies to facilitate the radiation or the emission of light [19].

## 2. Methods

The present work is carried out in THz frequency domain. The motivation of this choice is that in this domain only a few methods are available to steer and to control the flow of light. Thus, THz antennas are urgently needed for prospective applications. Moreover, since most of the envisioned THz devices serve for the purpose of sensing, antennas might meet exactly the needs for collecting and redirecting emission from localized sources as outlined in the introduction [20]. The present structures were fabricated by conventional photolithography on a silicon substrate (0.64-mm-thick, n-type, resistivity 12 Ωcm). The spirals with a C<sub>4</sub>-symmetry consist of wires with a width of 6 μm. The spiral is not circular but follows a rectangular shape. The arm length of the central wire was 30 μm. The length of the second winding was likewise 30 μm. The arm length of any additional winding was 24 μm more. All the geometrical parameters can be also extracted from Fig. 1 where the exact planar geometry of a spiral with

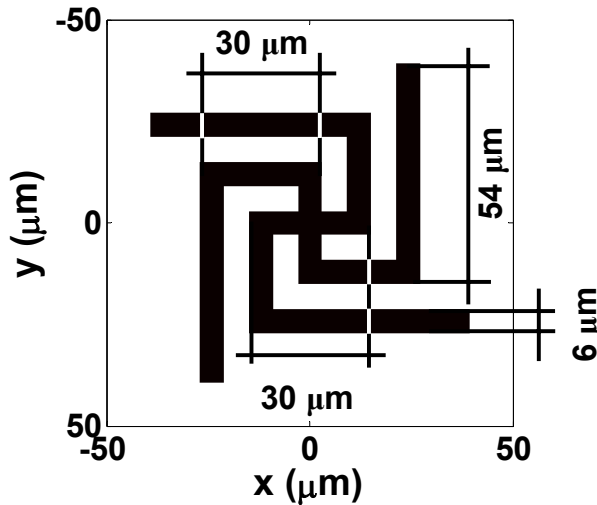


Fig. 1. Detailed geometrical parameters at the example of a THz spiral with three windings.

3 windings is shown. The spiral is fabricated using conventional photolithography technique and then depositing 200 nm of aluminum on the substrate. Spirals up to five windings were fabricated and characterized; although only selected results will be presented. To measure their optical properties and to access their resonant behavior, the spirals were arranged on a periodic lattice. The period for the sample with a single winding was 50  $\mu\text{m}$ . The period was gradually increased by 30  $\mu\text{m}$  for each additional winding. Microscopic images of relevant samples are shown in Fig. 2.

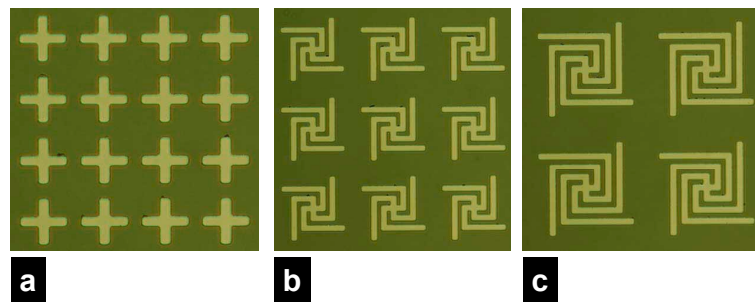


Fig. 2. Microscopic images of fabricated devices of the spiral type metamaterial with different winding numbers  $n$ ; (a)  $n = 1$ , (b)  $n = 3$ , (c)  $n = 4$ .

To measure the transmitted amplitude, a devoted broadband THz time-domain spectrometer (THz-TDS) was used [21]. It allows for the measurement of time traces of the amplitude of THz pulses transmitted through the sample [22]. By Fourier transforming this time trace, the spectral response is obtained. A normalization of this spectral response against the signal transmitted through a bare substrate allows access to the transmitted amplitude [23]. Most notably, with this method, the complex transmitted amplitude can be revealed. To allow for a comparison with theoretical predictions, we have been relying on the Fourier-modal method [24]. This numerical technique allows to solve the diffraction problem at bi-periodic gratings. To do so, all quantities of interest, such as the fields and the permittivity distribution of the structure are expanded in the

spatial Fourier domain. The solution consists then of two steps. At first, the eigenmodes inside the grating are expanded in a plane wave basis and solved by a devoted eigenvalue problem. At second, the amplitudes of all modes and of the transmitted and reflected plane waves are solved for by imposing appropriate boundary conditions to the interface between the incident and the grating domain as well as to the interface between the grating and the transmitted domain. In the simulation up to  $41 \times 41$  plane waves were retained along the truncation in the expansion of all relevant quantities. The entire geometry with nominal fabrication parameters was fully taken into account. Optical properties of Al were taken from literature and assumed to obey a Drude-like dispersion [25]. We assume throughout the manuscript that the illumination of the structure is at normal incidence with a linearly polarized plane wave.

### 3. Resonances of spiral type THz antennas

To start with, Fig. 3(a) shows the transmitted amplitude and Fig. 3(b) the transmitted phase through a spiral with only a single winding. The respective microscopic image of the pertinent structure was shown in Fig. 2(a). Results for both, simulation and experiment, are shown. We notice that the experiment and the simulation are in excellent agreement for both the amplitude and phase. From both spectra, we can observe a strong scattering response at a frequency of approximately 1.9 THz. The resonance corresponds to the fundamental eigenmode of a rectangular THz antenna. This rectangular THz antenna constitutes one of the two segments that form the spiral with a single winding. We proceed in using the term segment to describe the two elongated entities that form the spiral. Since the two segments for the respective spiral are mutually orthogonal to each other, their interaction can be understood as being negligible. The use of such a THz antenna to build a metamaterial would induce a strong dispersion in the effective permittivity.

To allow for a classification of the resonance we also evaluated the field distribution at the resonance frequencies. As usual, for the classification we rely on the amplitude of the normal component of the electric field shortly above the structure in reflection. However, it has to be mentioned that this choice is only for convenience. It was applied in former investigations to understand the characteristics and most notably to allow for a classification of the excited eigenmode [9]. It has to be mentioned that other quantities could have been used as well. The field distribution at a frequency of 1.9 THz is shown in Fig. 3(c). The dipolar character is clearly revealed. The amplitude possesses two lobes centered at the terminating end of the wire. The phase of the field associated with the two lobes has a difference of  $\pi$ . Along the line of the phase discontinuity the amplitude is zero. The amplitude possesses a single node, hence it is called the fundamental or first order mode. The current density associated with the resonance has a sinusoidal distribution with only half a period. It implies that the node in the pertinent field component is associated to the maximum of the current density.

Before proceeding to analyze the optical properties of spirals with a larger number of windings, we note that a spiral with two windings constitutes a gammadiion. It is an optical antenna that is quite well investigated since it allows for the observation of optical activity [26, 27]. Deposited on a dielectric substrate, it causes the rotation of the incident polarization due to quasi-planar chirality. Although the term has to be understood as an oxymoron, it is implied that the presence of the substrate breaks the mirror symmetry along the propagation direction which is the mandatory prerequisite for a structure to be called chiral [28]. Nonetheless, the optical activity of the present structure is negligible. The magnitude of the transmitted field component orthogonal to the incident one is three orders of magnitude less. The same holds for spirals with a larger number of windings which we proceed to analyze. A detailed analysis of optical activity in such structures is left for future work.

Figure 4 shows the measured and simulated spectral response of a spiral with three windings.

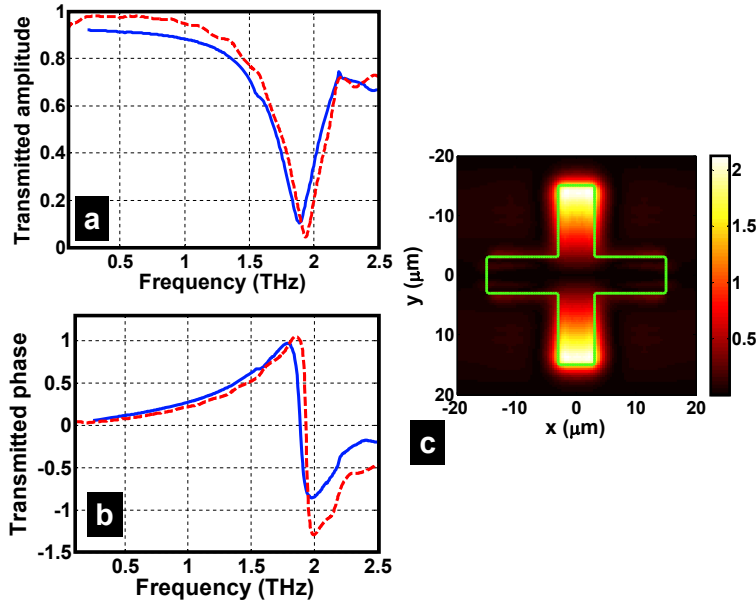


Fig. 3. Measured and simulated transmitted complex amplitude through a THz antenna sample comprising spirals with only a single winding where (a) shows the amplitude and (b) the phase. Blue solid and red dashed lines correspond to simulation and to measurement, respectively. The amplitude of the electric field component normal to the surface shortly above the structure is shown at the resonance frequency of 1.9 THz in (c). Polarization of the incident field is set to be in the  $y$ -direction.

Two strong resonances can be observed. They are labeled by roman figures. The resonance at the lower frequency (I) occurs at approximately 0.4 THz, whereas the resonance at the higher frequency occurs at approximately 1 THz. The shape of the latter resonance is slightly distorted due to the onset of a propagating diffraction order in the substrate. This occurs at rather low frequencies since the substrate has a large dielectric constant.

From the amplitude distribution of the normal component of the electric field above the structure [shown in Fig. 4(c)], it can be recognized that the resonance labeled as (I) constitutes the lowest order odd eigenmode of the THz antenna. It corresponds to the mode in the structure with a single winding. The eigenmode is characterized by a single amplitude node in the center of the structure and a strong field enhancement at the terminating ends of the spiral. The eigenmode is excited in both segments but with different magnitude. Although the incident polarization is chosen to be in the  $y$ -direction, the segment where the terminating arms are parallel to this direction appear only weakly excited. By contrast, the segment of the spiral having the terminating arms perpendicular to the incident polarization appears strongly excited. Such, at a first glance, counterintuitive behavior can be fairly simply understood by considering the overlap of the incident field with the distribution of the current density of the eigenmode. As stated before, it possesses a sinusoidal shape along each segment. The incident field is  $y$ -polarized and continuous over the entire surface of the spiral-type THz antenna where it may excite the respective eigenmode. A prerequisite for the excitation of the eigenmode is the need for a fraction of the segment to be aligned with the polarization of the incident wave field. Otherwise the mode cannot be excited. For this reason, e.g., only the segment aligned with the incident polarization was excited in the case for a spiral with a single winding. The opposite segment does not have any wire fraction that is aligned with the incident field. For the fundamental mode

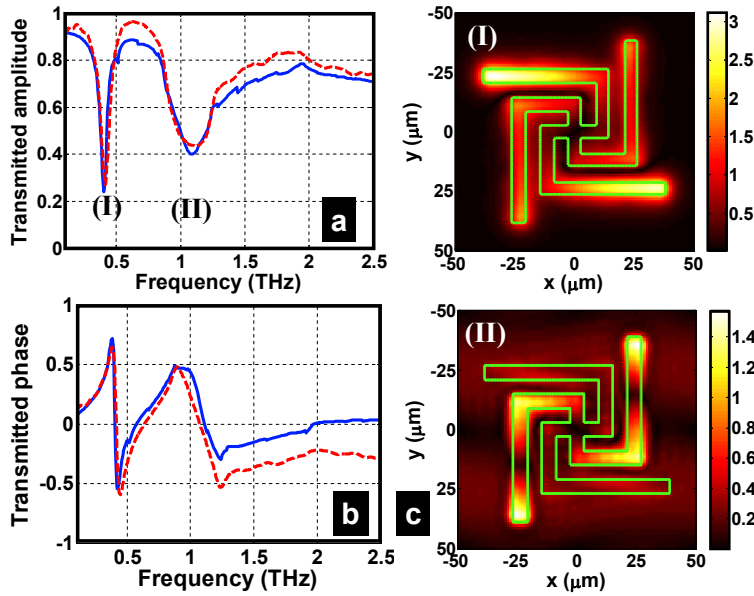


Fig. 4. Measured and simulated transmitted complex amplitude through a THz antenna sample composed of spirals with three windings where (a) shows the amplitude and (b) the phase, respectively. Blue solid and red dashed lines correspond to simulation and to measurement, respectively. For selected resonance frequencies, indicated by Roman numerals in (a), the amplitude of the electric field component normal to the surface shortly above the structure is shown in (c). Polarization of the incident field is set to be in the  $y$ -direction.

to be excited the central part of each segment is predominantly responsible. It occurs because the amplitude of the current density constituting the eigenmode is largest there. From Fig. 4(c) it can be seen that a larger part of the wire segment, where the eigenmode is strongly excited, meets this requirement and is consequently more strongly excited.

The opposite occurs at the second resonance labeled by (II) in Fig. 4(c). The mode is actually the third order eigenmode which can be seen from the three amplitude nodes across the segment. Along the lines of each amplitude nodal  $\pi$  phase jumps occur in the respective component of the electric field. The current density of the eigenmode has again a sinusoidal shape. One and a half period of such a sinusoidal function have to be considered. This eigenmode, therefore, has a strong amplitude component in the terminating fractions of the wires for each segment. Consequently, the segment is strongly excited where these wire elements are aligned with the incident polarization. Because of the  $C_4$  symmetry even order eigenmodes cannot be excited in the structure. Modifying the angle of incidence breaks this symmetry and even order modes might be excitable [29].

With an increasing number of windings no additional peculiarities with respect to the resonances are encountered. As can be seen for a spiral with four windings in Fig. 5, the excited eigenmodes cause deep and narrow dips in the transmission spectrum. The segments need to have a certain length to sustain the eigenmodes in the spectral domain of interest since they are associated with a standing wave pattern of the current density inside the metal. The effective wavelength does not strongly deviate from the free space wavelength since the metal behaves in this spectral domain as a near perfect conductor. For larger segments, a greater number of resonances are excited. For the spiral with four windings, up to three eigenmodes are clearly

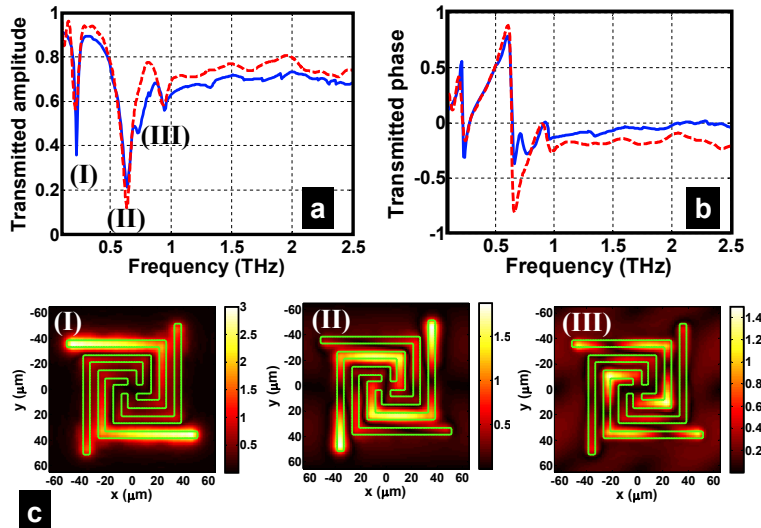


Fig. 5. Measured and simulated transmitted complex amplitude through a THz antenna sample composed of spirals with four windings where (a) shows the amplitude and (b) the phase, respectively. Blue solid and red dashed lines correspond to simulation and to measurement, respectively. For selected resonance frequencies, indicated by Roman numerals in (a), the amplitude of the electric field component normal to the surface shortly above the structure is shown in (c). Polarization of the incident field is set to be in the y-direction.

excitable. This can be seen from Figs. 5(a) and 5(b) where the amplitude and phase of the transmitted field are shown but also from (c) where the spatial amplitude distributions of the three lowest order resonances are displayed. The question as to which of the two segments is predominantly excited can again be best explained by considering the overlap of the incident field with the eigenmode, as carried out before in length. The only noticeable spectral feature is a steady convergence of the transmitted amplitude towards a constant value for larger frequencies.

#### 4. Manifestation of the Mushiake principle

Since in the analysis thus far we have only dealt with the amplitude of the 0<sup>th</sup> diffraction order in transmission, the question was open as into which directions light is steered by such structures at higher frequencies. To reveal these details, Fig. 6 shows the simulated reflected and transmitted intensity into the 0<sup>th</sup> diffraction order for the spiral-type THz antenna with four windings. Spectral properties of this sample were discussed before in Fig. 5. It shows furthermore the sum of both intensities. Note that we show the relative intensity rather than the amplitude as in the previous figures. It is obvious that in good approximation, the incident intensity is equally reflected and transmitted over a large spectral domain at higher frequencies. Remaining discrepancies are attributed at first to the intrinsic absorption in the dispersive material used for building the spiral-type THz antennas. However this accounts only for a few percent since the penetration depth of light in aluminum in the spectral domain of interest is negligible. At THz frequencies aluminum constitutes a nearly perfect conductor. The remaining energy that is not directly reflected or transmitted is therefore scattered into higher diffraction orders. Since the period is rather large compared to the relevant wavelengths in the material, various diffraction orders are propagating in either the substrate and/or the superstrate.

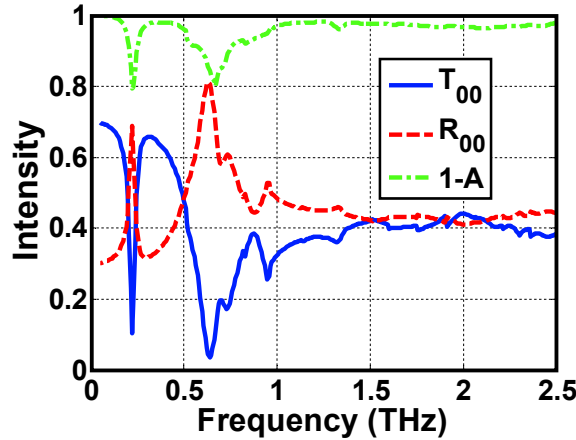


Fig. 6. Simulated transmitted (blue solid line) and reflected (red dashed) intensity diffracted into the lowest order (00). Unity minus the absorbed intensity is shown in addition (green dash-dotted line).

This equal partition of the intensity in reflection and transmission is the remarkable consequence of the Mushiake principle. The principle was originally introduced to explain the properties of certain self-complementary antennas operating at radio frequencies [17]. A self-complementary structure originates by rotating the original structure by  $90^\circ$  and a subsequent inversion. The latter implies an exchange of metal and air fraction of the structure. If this structure is identical to the original one it is called self-complementary. Ideal self-complementary two-port antennas have half the free space impedance. It results from an application of Babine's principle. Most notably, this property is independent of the frequency. We have to note that the pertinent spiral-type THz antennas are not exactly self-complementary. In their central portion as well as outside the actual spiral the structure deviates from this construction principle. A prototypical self-complementary spiral-type antennas would be, e.g., the Archimedan spiral with two arms. Nevertheless, the larger the number of windings the more negligible the deviations are.

Although spiral-type THz antennas with a large number of windings cannot be homogenized in a classical sense since their period is much larger than the wavelength, effective properties can be seemingly attributed to allow for an explanation of all observations. The structure acts like a frequency selective surface that has half the impedance of the free space. Although the translation of the concept for an impedance from radio to optical frequencies is somehow vague, the halving of the impedance seemingly causes a halving of the reflection and transmission for the frequency selective surface. This property occurs at frequencies much larger than the frequencies where the structure possesses a strong resonant response.

In contrast, wave optics provides a supplementary explanation for the observation that the transmitted and the reflected intensity coincide. The structure has obviously a peculiar geometry on a length scale much smaller than the wavelengths. The local structure of the spiral-type THz antenna constitutes a wire grid polarizer. Such a wire grid polarizer perfectly transmits TM- whereas it perfectly reflects TE-polarized light. Since the spiral is a wire grid polarizer where half the wires are aligned in  $x$ -direction and and  $y$ -direction, respectively, transmission through such a wire grid polarizer will be always 50% for a linearly polarized incidence. The spiral-type THz antennas must exhibit the effective properties of a diluted metal at these high frequencies. It allows half the intensity of the incident beam to be transmitted through the structure whereas the other half is reflected.

These features indicate that spiral-type THz antennas are interesting structures. Whereas they exhibit a response at shorter frequencies strongly affected by resonances, they can be reasonably described by a homogenized effective medium with negligible dispersion at higher frequencies. This could allow for potential applications as broadband and polarization insensitive attenuators or beam splitters at THz frequencies.

## 5. Conclusions

In conclusion, we have revealed the properties of spiral-type antennas. The investigation was done at THz frequencies; both experimentally and theoretically. At first we have studied the resonances in such structures. Their spectral appearance, the associated field distributions and their excitation strength were discussed. We proceeded in analyzing the properties of such antennas at larger frequencies. It was shown that the antennas equally divide the incident intensity into reflected and transmitted intensities. This is because of their geometry that is approximately self-complementary. Since this property is independent of the frequency, the structures are seemingly quite promising as potential optical elements in THz optical systems such as wave attenuators or splitters.

## Acknowledgements

The authors acknowledge Xinchao Lu for mask design and fruitful discussions with Jianqiang Gu, Zhen Tian, and Yongyao Chen. This work was partially supported by the US National Science Foundation, the German Federal Ministry of Education and Research (Metamat), the State of Thuringia (ProExzellenz Mema), the Tianjin Sci-Tech support program (Grant Nos. 07ZCGHHZ01100, 08ZCKFZC28000), and the National Basic Research Program of China (Grant No. 2007CB310403). Some computations utilized the IBM p690 cluster JUMP of the Forschungszentrum Jülich, Germany.